Proceedings of Science and Mathematics
Faculty of Science, Universiti Teknologi Malaysia
Vol. 18, 2023, page 127 – 135

Mathematical Modelling of Harmful Algal Blooms Using Nonlinear Ordinary Differential Equation

Sharisha Adira Sakawi, Normah Maan*
Department of Mathematical Sciences, Faculty of Science, Universiti Teknologi Malaysia
*Corresponding author: normahmaan@utm.my

Abstract
There has been an increase in occurrence of harmful algal blooms (HAB) reported over the last decade. HAB harms the ecosystem and can cause toxic effects on human and marine creatures. Some of the factors that influence the rise of HAB include nutrient availability, composition, and biotic factors such as competition and grazing. The purpose of this study is to formulate a mathematical model of zooplankton and phytoplankton relationship using ordinary differential equations. Phase portraits based on the mathematical model of the nonlinear zooplankton model system have been developed in this study to analyze the dynamical behaviors of the mathematical model. Results were compared between the critical points of the system which consisted of three equilibrium points. The linearization method is applied to the nonlinear differential equations to obtain the eigenvalues and eigenvectors for the equilibrium points. The phase portraits for each set of equilibrium points and eigenvectors are used to interpret and discuss the stability for the nonlinear ordinary differential equations.

Keywords: Harmful algal blooms; nonlinear ordinary differential equations; linearization; phase portraits

1. Introduction

Harmful algal bloom (HAB) refers to an occurrence that happens in natural marine or freshwater environments. This circumstance can be identified by a significant rise in the population of phytoplankton. The situation is also recognized as phytoplankton blooms, micro-algal blooms, toxic algae, red tides, and harmful. The proliferation of various phytoplankton species on the water surface disturbs the ecosystem and can have negative effects on humans, fish, and shellfish. This is mainly attributed to some microalgae that produce toxins, which can accumulate in shellfish and create a risk to human health when being consumed. Additionally, a certain types of microalgae species can cause fish mortality by clogging their gills, leading to lack of oxygen and subsequent death [8]. The presence of high level of density of algal blooms in water leads to a reduction in dissolved oxygen [19].

During the past decades, coastal region of the world have affected by harmful algal blooms seriously and causes massive losses in aquaculture, fisheries, human health, tourism, and ecosystems. Most HABs are caused by rapid proliferation of one or a few toxic or deleterious species of microalgae, although there is no universally accepted standard for the cell density that defines a bloom, as the blooming species and particularly its harmful effects. Studies on the negative effects of HABs have heretofore mainly focused on valuable animals and environmental factors such as dissolved oxygen and nutrients. However, investigations on the effect of HABs on plankton community structure and succession have been rare and were generally based on single trophic level and microscopic counting, except for one recent publication reporting the effects of a natural dinoflagellate bloom on the microbial community structure and succession via metagenomic approach [4].

As already mentioned earlier, HAB harms the ecosystem. The harm of microalgae can be easily seen by observing marine food resources. If marine food resources like aquaculture are affected, it can show the severity of the HAB. There are cases where some species are not visibly affected by the algae, but toxins accumulate in their organs. These toxins can be transmitted to humans through the consumption of contaminated seafood [8]. Some algal blooms are the result of an excess of nutrients, particularly phosphorus and nitrogen into water, and higher concentrations of these nutrients in water cause increased growth of algae and green plants. As more algae and plants grow, others die. This dead organic matter becomes food for bacteria that decomposes it. With more food available, the bacteria increase in number and use up the dissolved oxygen in the water. When the dissolved oxygen content decreases, many fish and aquatic insects can't survive. This results in dead area [6].

Some prior studies on harmful algal bloom have been conducted on the zooplankton – phytoplankton – fish model relation. There is a need to focus on the nonlinear ordinary differential equation system between zooplankton and phytoplankton with the growth rate of phytoplankton with the grazing rate of the zooplankton as the trigger mechanism, in which they are controlling the initiation of the outbreak and the refractory mechanism, which causes the model to return to its original state [6].

2. Nonlinear Ordinary Differential Equations

A complete nonlinear ordinary differential equation system for a zooplankton and phytoplankton relationship is derived based on the approach as presented by Nurul Huda Gazi and Kalyan Das (2010). The essence of the trigger mechanism assumed in our model lies in the interaction of the growth rate of phytoplankton with the grazing rate of the zooplankton. This is evidence that herbivore grazing plays a crucial role in the initial stages of a red tide outbreak. The rate of production of zooplankton, while their loss from the system is through death and natural predation by higher members of the food web, is via the consumption of the phytoplankton population. The model is given as

$$\frac{dx}{dt} = rx\left(1 - \frac{x}{K}\right) - R_m \frac{x^2}{a^2 + x^2} y, \tag{1}$$

$$\frac{dy}{dt} = -\mu y + bR_m \frac{x^2}{a^2 + x^2} y, \tag{2}$$

with the non-negative initial conditions given by $x(0) = x_0 > 0$ and $y(0) = y_0 > 0$.

The system above can be simplified as

$$\frac{dx}{dt} = xg(x) - yp(x), \tag{3}$$

$$\frac{dy}{dt} = y(h(x) - \mu) \tag{4}$$

with

$$g(x) = x\left(1 - \frac{x}{K}\right), \tag{5}$$

$$p(x) = R_m \frac{x^2}{a^2 + x^2}, \tag{6}$$

$$h(x) = bR_m \frac{x^2}{a^2 + x^2}, \tag{7}$$

where,

Table 1 Parameters for nonlinear equation

Parameters	Description
$x(t)$	Densities of phytoplankton in marine ecosystem
$y(t)$	Densities of zooplankton in marine ecosystem

$g(x)$	Growth rate of phytoplankton in absence of zooplankton
$p(x)$	Functional response of zooplankton
$h(x)$	Numerical response of zooplankton
r	Maximum growth rate
K	Carrying capacity
R_m	Maximum specific predation rate
a	How quickly maximum specific predation is attained as prey densities increase
μ	Rate of removal of zooplankton by death and predation
b	Ratio of biomass consumed to biomass of new herbivores produced

The nonlinear ODE is a prey and predator model system with zooplankton as the prey, and phytoplankton as the predator. There are some assumptions that can be made from the model. In the absent of phytoplankton, the population of zooplankton will grow at the natural rate, $\frac{dx}{dt} = xg(x),\ g(x) > 0$. Meanwhile, in the absent of zooplankton, the population of phytoplankton could decrease at the natural rate, $\frac{dy}{dt} = -\mu y,\ \mu > 0$. The present of both zooplankton and phytoplankton is beneficial for the growth of the population of phytoplankton and is harmful for the growth of the population of zooplankton.

3. Linearization of Nonlinear ODEs

In this section, linearization is used to analyze the system. The parameters $g(x)$, $h(x)$, $p(x)$, and μ are assumed to be positive. This system represents the predator-prey relationship between zooplankton and phytoplankton where the variables x and y are restricted to be nonnegative. In this context, the system is known as the Lotka-Volterra equations.

To analyze the system, the first step is to find the critical points of the system. By referring to the zero isoclines of the model system yield three equilibrium points which are $(0,0)$, $(K,0)$, and $E(x_*, y_*)$ where x_*, y_* are given by

$$x_* = \frac{a\sqrt{\mu}}{\sqrt{bR_m - \mu}} \tag{8}$$

and

$$y_* = \frac{br}{\mu}\left[1 - \frac{x_*}{K}\right]x_*. \tag{9}$$

By applying the linearization in equation (1) and (2) at those points, one can observe the approximate behavior of the solutions over time when an initial condition is close to the equilibrium points. We start by computing the derivative matrix

$$DF(x,y) = \begin{pmatrix} r - \frac{2rx}{K} - R_m y\left(\frac{2x^3 - 2x(a^2+x^2)}{a^2+x^2}\right) & -R_m\frac{x^2}{a^2+x^2} \\ bR_m y\left(\frac{2x^3 - 2x(a^2+x^2)}{a^2+x^2}\right) & -\mu + b\frac{R_m x^2}{a^2+x^2} \end{pmatrix} \tag{10}$$

The linearization at the equilibrium solution (0,0) is given by

$$DF(0,0) = \begin{pmatrix} r & 0 \\ 0 & -\mu \end{pmatrix} = A \tag{11}$$

The matrix A in (11) is then subtracted with λI in which $\lambda I = \begin{pmatrix} \lambda & 0 \\ 0 & \lambda \end{pmatrix}$

$$A - \lambda I = \begin{pmatrix} r & 0 \\ 0 & -\mu \end{pmatrix} - \begin{pmatrix} \lambda & 0 \\ 0 & \lambda \end{pmatrix} \tag{12}$$

This will give the matrix

$$\begin{pmatrix} r-\lambda & 0 \\ 0 & -\mu-\lambda \end{pmatrix} \tag{13}$$

From the equation acquired in (13), the determinant can be searched by

$$det \begin{pmatrix} r-\lambda & 0 \\ 0 & -\mu-\lambda \end{pmatrix} \tag{14}$$

Solving the equation in (14) will give

$$(r-\lambda)(-\mu-\lambda) \tag{15}$$

By having the equation in (15) equal to 0, two values of λ are obtained

$$\lambda = r, \lambda = -\mu \tag{16}$$

Then, the linearization at the equilibrium solution $(K, 0)$ is given by

$$DF(K,0) = \begin{pmatrix} -r & -R_m \dfrac{K^2}{a^2+K^2} \\ 0 & -\mu + b\dfrac{R_m K^2}{a^2+K^2} \end{pmatrix} = B \tag{17}$$

The matrix B in (4.17) is then subtracted with λI

$$B - \lambda I = \begin{pmatrix} -r & -R_m \dfrac{K^2}{a^2+K^2} \\ 0 & -\mu + b\dfrac{R_m K^2}{a^2+K^2} \end{pmatrix} - \begin{pmatrix} \lambda & 0 \\ 0 & \lambda \end{pmatrix} \tag{18}$$

This will give the matri

$$\begin{pmatrix} -r-\lambda & -R_m \dfrac{K^2}{a^2+K^2} \\ 0 & -\mu + b\dfrac{R_m K^2}{a^2+K^2} - \lambda \end{pmatrix} \tag{19}$$

From the equation acquired in (4.19), the determinant can be searched by

$$\det \begin{pmatrix} -r-\lambda & -R_m \dfrac{K^2}{a^2+K^2} \\ 0 & -\mu + b\dfrac{R_m K^2}{a^2+K^2} - \lambda \end{pmatrix} \tag{20}$$

Solving the equation in (20) will give

$$(-r-\lambda)\left(-\mu + b\frac{R_m K^2}{a^2+K^2} - \lambda\right) \tag{21}$$

By having the equation in (21) equal to 0, two values of λ are obtained

$$\lambda = -r, \lambda = -\mu + b\frac{R_m K^2}{a^2+K^2} \tag{22}$$

Lastly, the linearization at the equilibrium solution $E_*(x_*, y_*)$ is given by

$DF((x_*, y_*) =$

$$\begin{pmatrix} r - \frac{2r}{K}x_* - R_m y_* \left(\frac{2x_*^3 - 2x_*(a^2 + x_*^2)}{(a^2 + x_*^2)^2}\right) & -R_m \frac{x_*^2}{a^2 + x_*^2} \\ bR_m y_* \left(\frac{2x_*^3 - 2x_*(a^2 + x_*^2)}{(a^2 + x_*^2)^2}\right) & -\mu + b\frac{R_m x_*^2}{a^2 + x_*^2} - \lambda \end{pmatrix} = C \tag{23}$$

The matrix B in (23) is then subtracted with λI

$$C - \lambda I = \begin{pmatrix} r - \frac{2r}{K}x_* - R_m y_* \left(\frac{2x_*^3 - 2x_*(a^2 + x_*^2)}{(a^2 + x_*^2)^2}\right) & -R_m \frac{x_*^2}{a^2 + x_*^2} \\ bR_m y_* \left(\frac{2x_*^3 - 2x_*(a^2 + x_*^2)}{(a^2 + x_*^2)^2}\right) & -\mu + b\frac{R_m x_*^2}{a^2 + x_*^2} - \lambda \end{pmatrix} - \begin{pmatrix} \lambda & 0 \\ 0 & \lambda \end{pmatrix} \tag{24}$$

This will give the matrix

$$\begin{pmatrix} r - \frac{2r}{K}x_* - R_m y_* \left(\frac{2x_*^3 - 2x_*(a^2 + x_*^2)}{(a^2 + x_*^2)^2}\right) - \lambda & -R_m \frac{x_*^2}{a^2 + x_*^2} \\ bR_m y_* \left(\frac{2x_*^3 - 2x_*(a^2 + x_*^2)}{(a^2 + x_*^2)^2}\right) & -\mu + b\frac{R_m x_*^2}{a^2 + x_*^2} - \lambda \end{pmatrix} \tag{25}$$

From the equation acquired in (25), the determinant can be searched by

$$\det \begin{pmatrix} r - \frac{2r}{K}x_* - R_m y_* \left(\frac{2x_*^3 - 2x_*(a^2 + x_*^2)}{(a^2 + x_*^2)^2}\right) - \lambda & -R_m \frac{x_*^2}{a^2 + x_*^2} \\ bR_m y_* \left(\frac{2x_*^3 - 2x_*(a^2 + x_*^2)}{(a^2 + x_*^2)^2}\right) & -\mu + b\frac{R_m x_*^2}{a^2 + x_*^2} - \lambda \end{pmatrix} \tag{26}$$

Solving the equation in (26) will give

$$\lambda = \frac{-\mu + x_* + x_*^2\left(\frac{bR_m}{a^2 + x_*^2} - \frac{1}{K}\right) \pm \sqrt{p}}{2} \tag{4.27}$$

with

$$p = \frac{bR_m x_*^2}{a^2 + x_*^2}\left[bR_m x_*^2 - 2\mu + 2x\left(1 - \frac{x}{K}\right)\right] + x_*^2\left[1 - \frac{-2x}{K} + \frac{x_*^2}{K^2}\right] - 2\mu x(1 - \frac{x}{K})$$

3.1 Solution for Nonlinear Ordinary Differential Equations

By taking these values, the nonlinear ordinary differential equations presumably become as below.

Table 2 : Values for zooplankton phytoplankton model [18]

Parameter	Description	Value	Unit
r	Maximum growth rate	0.3	d^{-1}
R_m	Maximum specific predation rate	0.7	d^{-1}
a	How quickly maximum specific predation is attained as prey densities increase	2.0	-
b	Ratio of biomass consumed to biomass of new herbivores produced	0.02	-
μ	Rate of removal of zooplankton by death and predation	0.001-0.035	d^{-1}
K	Carrying capacity	108	$\mu g N l^{-1}$

$$\frac{dx}{dt} = x^2 - \frac{x^3}{108} - 0.7\frac{x^2}{4+x^2}y \tag{28}$$

$$\frac{dy}{dt} = -0.001y + \frac{0.014x^2}{4+x^2}y \tag{29}$$

The critical points become $(0,0)$, $(108,0)$, and $E(0.5547,3.3111)$, each with their own set of expected eigenvalues and eigenvectors. The eigenvectors are used to create phase portraits for the equilibrium points, which show the direction and magnitude of the solutions. Analysis of the phase portraits tell the locations, types of equilibria and the general shapes of the solutions near those equilibria.

The linearization at the equilibrium solution $(0,0)$ is given by $DF(0,0)$, $\begin{pmatrix} u' \\ v' \end{pmatrix} = \begin{pmatrix} -0.001 & 0 \\ 0 & 0.3 \end{pmatrix}\begin{pmatrix} u \\ v \end{pmatrix}$. The eigenvalues for this system, then are $\lambda_1 = -0.001$ and $\lambda_2 = 0.3$ and the eigenvectors are $\begin{pmatrix} 0 & 1 \\ 1 & 0 \end{pmatrix}$. One eigenvalue is positive and the other is negative.

At the point $(108,0)$, the system can be analysed in a similar fashion. The linearized system is $\begin{pmatrix} \mathrm{u}' \\ \mathrm{v}' \end{pmatrix} = \begin{pmatrix} -0.3 & 0 \\ 0 & 0.013 \end{pmatrix}\begin{pmatrix} \mathrm{u} \\ \mathrm{v} \end{pmatrix}$, for which the eigenvalues are $\lambda_1 = -0.3$ and $\lambda_2 = 0.013$ and the eigenvectors are $\begin{pmatrix} 1 & -0.9129 \\ 0 & 0.4083 \end{pmatrix}$.

At the point $(0.5447,3.3111)$, the system can be analysed in a similar fashion. The linearized system is $\begin{pmatrix} \mathrm{u}' \\ \mathrm{v}' \end{pmatrix} = \begin{pmatrix} 0.4655 & 0 \\ 0 & -0.0012 \end{pmatrix}\begin{pmatrix} \mathrm{u} \\ \mathrm{v} \end{pmatrix}$, for which the eigenvalues are $\lambda_1 = 0.4655$ and $\lambda_2 = -0.0012$ with $\begin{pmatrix} 0.9997 & 0.1068 \\ -0.0238 & 0.9943 \end{pmatrix}$ as the eigenvectors.

3. Results and discussion

The eigenvectors for each set of equilibrium points are used to plot the phase portrait. The phase portrait depicted in Figure 4.1 shows the phase portrait for equilibrium solution $(0,0)$. The system has two eigenvectors $\begin{pmatrix} 0 \\ 1 \end{pmatrix}$ and $\begin{pmatrix} 1 \\ 0 \end{pmatrix}$. Only trajectories along $\begin{pmatrix} 1 \\ 0 \end{pmatrix}$ are stable trajectories, while the other trajectories at start are tangent to $\begin{pmatrix} 1 \\ 0 \end{pmatrix}$ and later are tangent to $\begin{pmatrix} 0 \\ 1 \end{pmatrix}$. This equilibrium point is unstable and referred to as a saddle point.

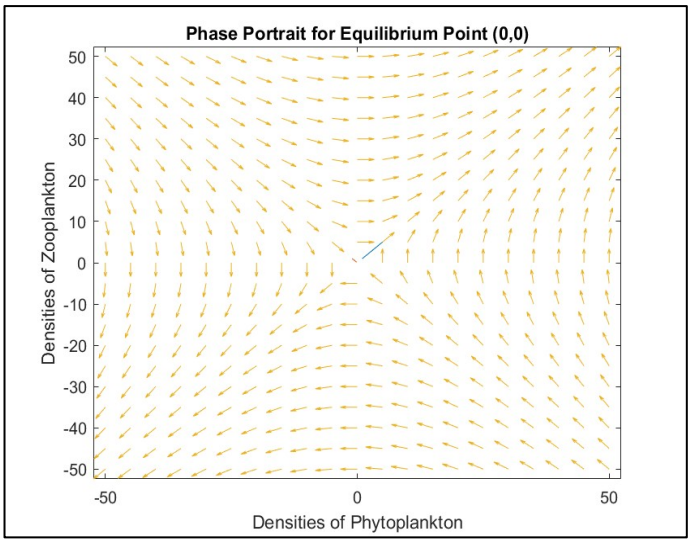

Figure 1 Phase Portrait for equilibrium point (0,0)

The equilibrium point $(108,0)$ is an unstable node and referred to as source point. The system has two eigenvectors $\begin{pmatrix}-0.3\\0\end{pmatrix}$ and $\begin{pmatrix}0\\0.013\end{pmatrix}$. The phase portrait has trajectories that are tangent to the slow eigenvector $\begin{pmatrix}-0.3\\0\end{pmatrix}$ for near origin, and parallel to the fast eigenvector $\begin{pmatrix}0\\0.013\end{pmatrix}$ for far from origin.

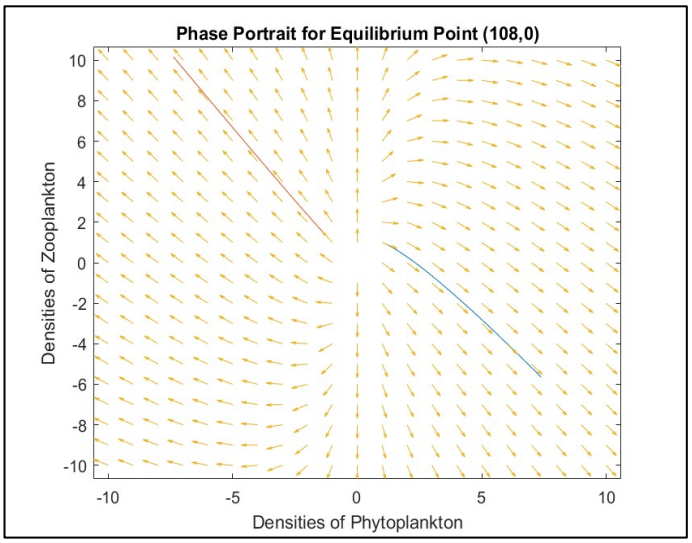

Figure 2 Phase portrait for equilibrium point (108,0)

The equilibrium point $(0.5547,3.3111)$ has two eigenvectors which are $\begin{pmatrix}0.9997\\-0.0238\end{pmatrix}$ and $\begin{pmatrix}0.1068\\0.9943\end{pmatrix}$. The trajectories are all along the initial conditions and they are outward the origin.

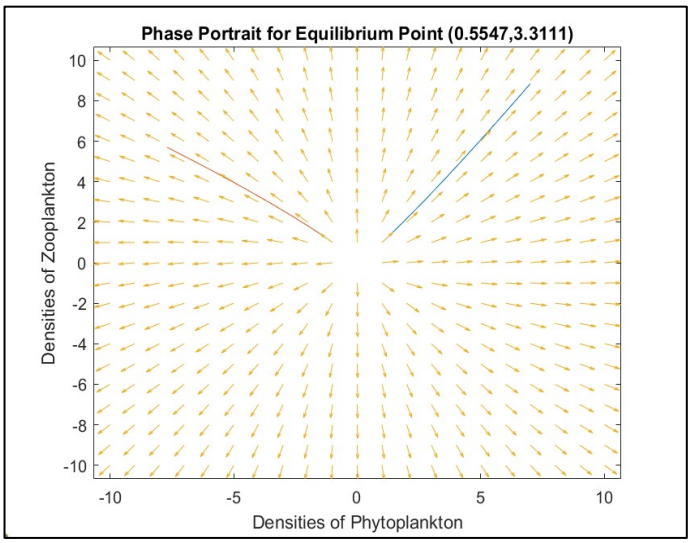

Figure 3 Phase portrait for equilibrium point (0.5547, 3.3111)

Conclusion

The objectives of this project have been achieved. The mathematical model of zooplankton phytoplankton relationship has been formulated by using nonlinear ordinary differential equations.

The two-dimensional nonlinear ordinary differential equations are used to develop a mathematical model for the interaction between zooplankton and phytoplankton. By using the linearization method on the nonlinear ordinary differential equations, equilibrium points, eigenvalues and eigenvectors are obtained. The eigenvectors for each set of equilibrium points are used to plot the phase portraits of the mathematical model of the nonlinear zooplankton phytoplankton model system. The phase portraits have

been constructed by using Matlab-Simulink platform which is used to analyze the dynamical behaviors of the mathematical model. From the result obtained from the previous chapter, it can be seen that the nonlinear ordinary differential equations of the zooplankton phytoplankton model are unstable.

References

[1] Jipanin, S. J., Muhamad Shaleh, S. R., Lim, P. T., Leaw, C. P., & Mustapha, S. (2019). The Monitoring of Harmful Algae Blooms in Sabah, Malaysia. *Journal of Physics: Conference Series*, *1358*(1). https://doi.org/10.1088/1742-6596/1358/1/012014

[2] Yussof, F. N., Maan, N., Md Reba, M. N., & Khan, F. A. (2022). Mathematical Modelling of Harmful Algal Blooms on West Coast of Sabah. *Mathematics*, *10*(16). https://doi.org/10.3390/math10162836

[3] Nonlinear Systems Analysis 1. Phase-Plane Analysis. (2004). Cheric. Retrieved June 10, 2023, from https://www.cheric.org/files/education/cyberlecture/d200401/d200401-501.pdf

[4] Mercado, J. M., Cortés, D., Gómez-Jakobsen, F., García-Gómez, C., Ouaissa, S., Yebra, L., Ferrera, I., Valcárcel-Pérez, N., López, M., García-Muñoz, R., Ramos, A., Bernardeau, J., Belando, M. D., Fraile-Nuez, E., & Ruíz, J. M. (2021). Role of small-sized phytoplankton in triggering an ecosystem disruptive algal bloom in a Mediterranean hypersaline coastal lagoon. *Marine Pollution Bulletin*, *164*. https://doi.org/10.1016/J.MARPOLBUL.2021.111989

[5] Chakraborty, S., Moorthi, S. D., Karnatak, R., & Feudel, U. (2022). Irregular harmful algal blooms triggered by feedback between toxin production and zooplankton feeding. Ecological Modelling, 473. https://doi.org/10.1016/J.ECOLMODEL.2022.110120

[6] Gazi, N. H., & Das, K. (2010). Structural stability analysis of an algal bloom mathematical model in tropic interaction. Nonlinear Analysis: Real World Applications, 11(4), 2191–2206. https://doi.org/10.1016/J.NONRWA.2009.06.009

[7] Fisheries dept: Toxic algal bloom caused the death of fish in Penang, Perak. (2020). Retrieved June 10, 2023, from https://www.thesundaily.my/local/fisheries-dept-toxic-algal-bloom-caused-the-death-of-fish-in-penang-perak-XA2516365

[8] What are Harmful Algae - Harmful Algal Bloom Programme. (2021). Retrieved November 21, 2022, from https://hab.ioc-unesco.org/what-are-harmful-algae/

[9] Pal, M., Yesankar, P. J., Dwivedi, A., & Qureshi, A. (2020). Biotic control of harmful algal blooms (HABs): A brief review. Journal of Environmental Management, 268. https://doi.org/10.1016/J.JENVMAN.2020.110687

[10] Lomartire, S., Marques, J. C., & Gonçalves, A. M. M. (2021a). The key role of zooplankton in ecosystem services: A perspective of interaction between zooplankton and fish recruitment. Ecological Indicators, 129. https://doi.org/10.1016/J.ECOLIND.2021.107867

[11] Ersoy, Z., Brucet, S., Bartrons, M., & Mehner, T. (2019). Short-term fish predation destroys resilience of zooplankton communities and prevents recovery of phytoplankton control by zooplankton grazing. PLOS ONE, 14(2), e0212351. https://doi.org/10.1371/JOURNAL.PONE.0212351

[12] Zohdi, E., & Abbaspour, M. (2019). Harmful algal blooms (red tide): a review of causes, impacts and approaches to monitoring and prediction. International Journal of Environmental Science and Technology, 16(3), 1789–1806. https://doi.org/10.1007/S13762-018-2108-X/TABLES/4

[13] Coyne, K. J., Wang, Y., & Johnson, G. (2022). Algicidal Bacteria: A Review of Current Knowledge and Applications to Control Harmful Algal Blooms. In Frontiers in Microbiology (Vol. 13). Frontiers Media S.A. https://doi.org/10.3389/fmicb.2022.871177

[14] Kaur, R. P., Sharma, A., & Sharma, A. K. (2021). Impact of fear effect on plankton-fish system dynamics incorporating zooplankton refuge. Chaos, Solitons and Fractals, 143. https://doi.org/10.1016/J.CHAOS.2020.110563

[15] Morgan, R. (2015). Issue 2 Article 5 Recommended Citation Recommended Citation Morgan. In Undergraduate Mathematics Journal Rose-Hulman Undergraduate Mathematics Journal (Vol. 16, Issue 2).

[16] Phytoplankton | MIT Climate Portal. (2022). Retrieved November 21, 2022, from https://climate.mit.edu/explainers/phytoplankton
[17] Stability and Phase Plane Analysis Advanced Control (Mehdi Keshmiri, Winter 95). (2017).
[18] Woodward, J. R., Pitchford, J. W., & Bees, M. A. (2019). Physical flow effects can dictate plankton population dynamics. Journal of the Royal Society Interface, 16(157). https://doi.org/10.1098/rsif.2019.